FULL PAPER

Embossed Hollow Hemisphere-Based Piezoelectric Nanogenerator and Highly Responsive Pressure Sensor

Jinsung Chun, Keun Young Lee, Chong-Yun Kang, Myung Wha Kim, Sang-Woo Kim, and Jeong Min Baik**

Harvesting energy using piezoelectric materials such as ZnO, at nanoscale due to geometrical effects, are highly desirable for powering portable electronics, biomedical, and healthcare applications. Although one-dimensional nanostructures such as nanowires have been the most widely studied for these applications, there exist a limited number of piezomaterials that can be easily manufactured into nanowires, thus, developing effective and reliable means of preparing nanostructures from a wide variety of piezomaterials is essential for the advancement of self-powered devices. In this study, ZnO embossed hollow hemispheres thin film for highly responsive pressure sensors and nanogenerators are reported. The asymmetric hemispheres, formed by an oblique angle deposition, cause an unsymmetrical piezoelectric field direction by external force, resulting in the control of the current direction and level at about 7 mA cm^{-2} at normal force of 30 N. The nanogenerators repeatedly generate the voltage output of ≈0.2 V, irrespective of the degree of symmetry. It is also demonstrated that when one piece of hemisphere layer is stacked over another to form a layer-by-layer matched architecture, the output voltage in nanogenerators increases up to 2 times.

1. Introduction

Energy harvesting technologies may meet critical demand in areas where alternatives to fossil fuels are required for environmental protection, and in portable applications that require super-high energy capacity or complementary energy sources. Harvesting energy from ambient energy sources including solar,[1–8] thermal,[9] and mechanical energy,[10–18] has attracted intensive interest in the past years to meet these needs. Among these, piezoelectric harvesting technology,[12,14,19,20] which converts mechanical energy, the most common energy source available anywhere at any time, into electrical energy, has been proposed and investigated by many researchers because of an extended life time, no recharging procedures, and scalability. To date, there have been attempts to fabricate piezoelectric energy harvesting devices, named as nanogenerators, by employing various piezoelectric nanostructures including nanowires,[14,21–24] nanotubes,[25] and porous structures,[26] in which most works have been focused on nanowire-type generators. However, these technologies still suffer from many drawbacks that limit the successful commercialization. Recently, thin film-type nanogenerators with perovskite ceramic materials ($BaTiO_3$ and $ZnSnO_3$)[27,28] were also demonstrated, generating a much higher level of power density than other similar structural or related devices.

The advent of nanogenerator and nanotechnology may significantly lead to a self-powered system, based on driving portable devices with low power consumption by harvesting energy from ambient energy sources. Recent development in sensor technologies has provided innovative ways to reduce power consumption up to less than 1 mW,[29,30] enough to be produced by nanogenerators. Nanogenerator-assisted self-powered magnetic,[31] chemical,[32] temperature,[33] and mechanical sensors[34] have been successfully demonstrated. This approach can greatly enhance the adaptability, mobility, and durability of such sensors. Here, we introduce highly-ordered embossed thin films with hollow hemispheres as one of promising structures for nanogenerators and pressure sensors, produced by a spin coating of two-dimensional polystyrene spheres on planar substrates, followed by the deposition of ZnO layer by a radio-frequency magnetron sputtering method at room temperature and post-annealing.

J. Chun, Prof. J. M. Baik
School of Mechanical and Advanced Materials Engineering
KIST-UNIST-Ulsan Center for Convergent Materials
Ulsan National Institute of Science and Technology (UNIST)
Ulsan, 689-798, Republic of Korea
E-mail: jbaik@unist.ac.kr
K. Y. Lee, Prof. S.-W. Kim
School of Advanced Materials Science and Engineering
Sungkyunkwan University (SKKU)
Suwon, 440-746, Republic of Korea
E-mail: kimsw1@skku.edu

DOI: 10.1002/adfm.201302962

Dr. C.-Y. Kang
Electronic Materials Research
Center, KIST, Hwarangno 14-gil 5, Seongbuk-gu,
Seoul, 137-791, Republic of Korea
KU-KIST Graduate School of Converging Science and Technology
Korea University
145, Anam-ro, Seongbuk-gu, Seoul, 136-701, Korea., Republic of Korea
Prof. M. W. Kim
Department of Chemistry & Nano Science
Ewha Womans University
Seoul, 120-750, Republic of Korea

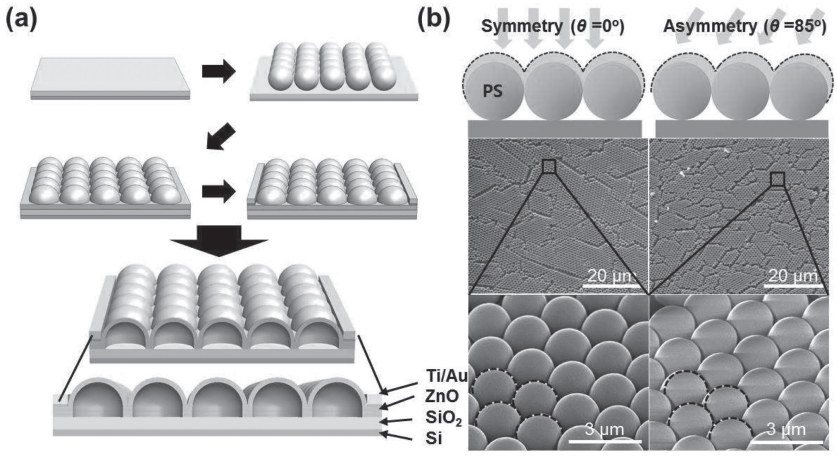

Figure 1. a) Schematic diagrams of the pressure sensor fabrication process. b) Hexagonally close-packed 2D arrays as a form of multi-domains of areas larger than approximately 20 μm^2. Oblique angle deposition of ZnO ($\theta = 85°$) produced asymmetric hemispheres.

Our approach has the advantages of quasi-ordered 2D films with large dimension (>280 cm^2 area),[35] precisely controlled multilayer structures via physical vapor deposition, and no limitation on materials. The embossed thin film also has a high mechanical durability with good stretchable properties, compared with conventional thin film.

Upon subsequent removal of the organic template by thermal decomposition, the ZnO film exhibits a macro-porous structure with hollow hemispheres. For pressure sensors, laterally aligned electrodes were formed by deposition of Ti/Au and indium wire bonding, while vertically arranged electrodes (ITO) on the top and bottom of the embossed hemispheres were used in the nanogenerator (detailed information is described in the experimental section). For enhancing the performance of the pressure sensors, we employed an oblique angle deposition (OAD) technique which makes the hemispheres asymmetric. However, it is also demonstrated that the OAD does not enhance the performance of the nanogenerator.

2. Results and Discussion

The schematic diagrams of the pressure sensor fabrication process are shown in **Figure 1**a and detailed information described in Experimental section. Scanning electron microscopy (SEM) images in Figure 1b shows that the 2D ZnO hollow hemisphere arrays are hexagonally close-packed as a form of multi-domains of areas larger than approximately 20 μm^2. By a spin coating method of PS spheres, quasi-continuous 2D array monolayers which fill the entire substrate of >10 cm^2 area are studied in the current study. By heating at 300 °C for 1 h in air, it produces ZnO embossed thin films with hemispheres, well-distributed on the substrates.

The microstructure and crystalline properties of the embossed ZnO thin films were characterized by transmission electron microscopy (TEM) and X-ray diffraction (XRD). In the XRD spectrum (**Figure 2**a), there is only one peak corresponding to the (0002) plane of ZnO, showing preferred orientation of ZnO thin films. As the angle between substrate normal and vapor flux increases, the peak shifts to the higher angle by 0.3° and the full-width-half-maximum (FWHM) decreases from 0.32° to 0.3°, meaning an improvement in the crystallinity of the embossed films deposited by OAD. Figure 2b shows a cross-sectional TEM image of asymmetric hemispheres, which reveals that the hemispheres are hollow. Clearly, a film was deposited directly on the substrate although the bottoms of the hemispheres fold into the hollow inner space. The elemental maps, determined by energy dispersive X-ray (EDX), of an embossed ZnO thin film confirms the formation of asymmetric hemispheres consisting of Zn and O atoms. The high-resolution TEM (HR-TEM) images show that the film clearly reveals columnar structures with grain sizes in the range of 10–20 nm. Each grain seems to be highly crystalline, based on the facts that the most part of the domains is bright in dark field image, lattice fringes are well ordered. Furthermore, high magnification at the domain interface clearly shows the crystalline continuity between the grains, indicating that the embossed ZnO films enable reliable device action. It can also be seen that there are some stacking faults at the interface since the grains are fan-shaped (it means that the grain size increases from bottom to top).

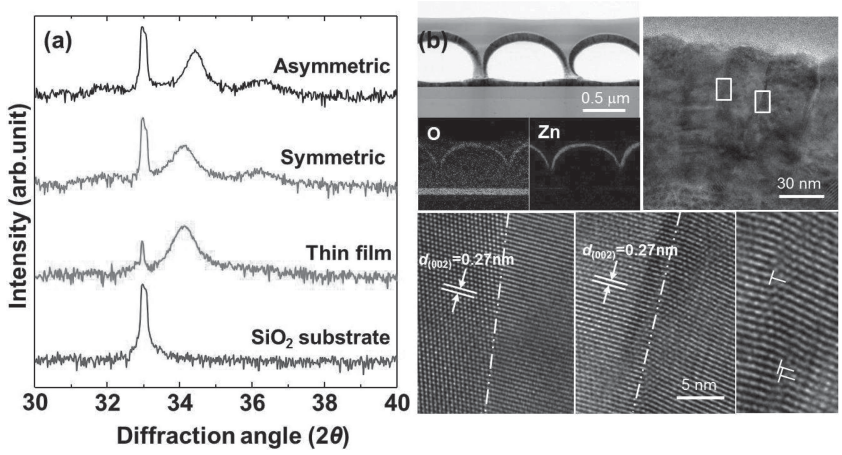

Figure 2. a) The XRD patterns of ZnO thin films with symmetric and asymmetric hollow hemispheres on SiO_2/Si substrate. b) A cross-sectional TEM image and EDX results of asymmetric shaped hemispheres, which reveals that the hemispheres are hollow and consist of Zn and O atoms. The HR-TEM images also show that the hemisphere has columnar structures with grain sizes in the range of 10–20 nm. High crystallinity of each grain, based on facts that the most part of the grains is bright in dark field image and lattice fringes are well ordered.

Figure 3a shows the change of the current density with the applied voltage of 10 mV when the external force of 30 N is applied. For

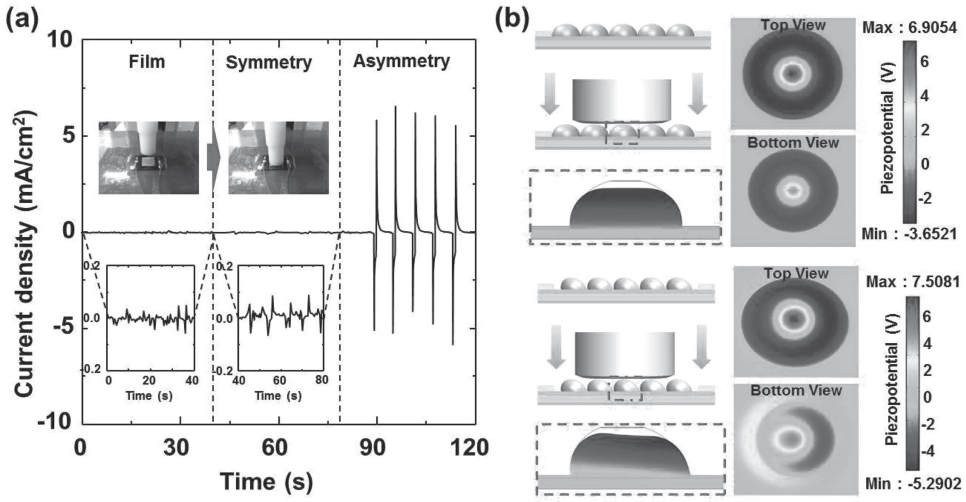

Figure 3. a) The change of the current density with the applied voltage of 10 mV when the external force of 30 N is applied and b) piezoelectric potential distributions inside a hemisphere along the direction (transverse and vertical) for symmetric (top) and asymmetric (bottom) hollow hemispheres.

thin film and embossed thin film with symmetric hemispheres, there is no change in the current density when we push the samples, as shown in the inset, although there is a little change (<0.05 mA cm^{-2}) in the embossed film by the force. By making the hemispheres asymmetric, a sharp current pulse up to 7 mA cm^{-2} was clearly observed when the sample was pushed quickly. The unsymmetrical pressure between the tensile and compressive stressed region in hemispheres along lateral direction causes a gradient in the piezoelectric potential, resulting in the control of the current direction and level to be approximately 7 mA cm^{-2} at the normal force of 30 N. If the sensitivity of the pressure sensor is defined to be $S = (I_p - I_o)/I_o p$, where p denotes the applied pressure, I_p and I_o denote the current with and without applied pressure, the sensitivity of the sensor with asymmetric hemispheres is calculated to be 1.64 kPa^{-1}, higher than those of film and symmetric hemispheres. The change of current density by a pushing force in embossed films with hollow hemispheres can be understood from the piezoelectric potential distributions inside a hemisphere along the direction (Figure 3b). A COMSOL package was used to investigate the piezoelectric potential distribution inside the hemisphere. In case of the thin film, it is not likely to deform by such pushing force, evident by no change of current density. The asymmetric hemisphere causes an unsymmetrical strain distribution along the transverse direction due to the pushing force. Specifically, strain gradient is dominant and the stress is dominantly distributed at the bottom area of the thicker hemisphere (see left side at near bottom of the hemisphere). The gradient of the piezoelectric potential near the bottom of the hemisphere resulted in a net electrical field along the transverse direction. However, for a symmetric hemisphere, the electric field direction and the piezoelectric potential by external force are seen to be same, resulting in a zero net electric field and no change of current density.

When a measurement instrument is forward connected to the device, the device showed a positive current upon the pushing states (**Figure 4**). In the case of the reverse connection, the negative current pulses are measured. This result indicates that the measured current are the true signals generated from the devices strained by pushing motions. **Figure 5** also shows

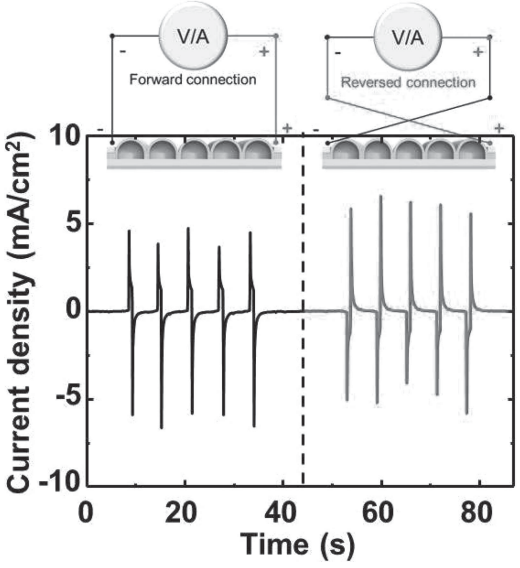

Figure 4. The output current signals of the embossed thin film measured in the forward connection and in the reverse connection.

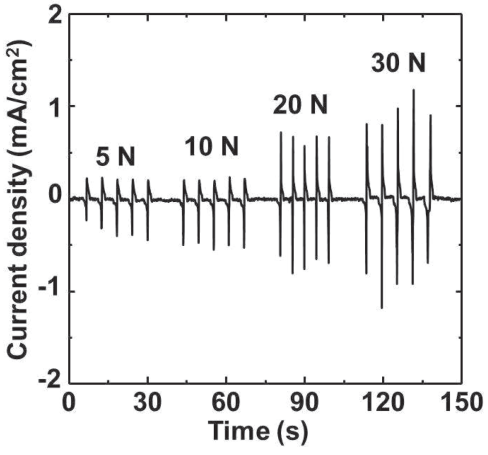

Figure 5. The change of current density of the sensor with the magnitude of applied forces (5, 10, 20, and 30 N).

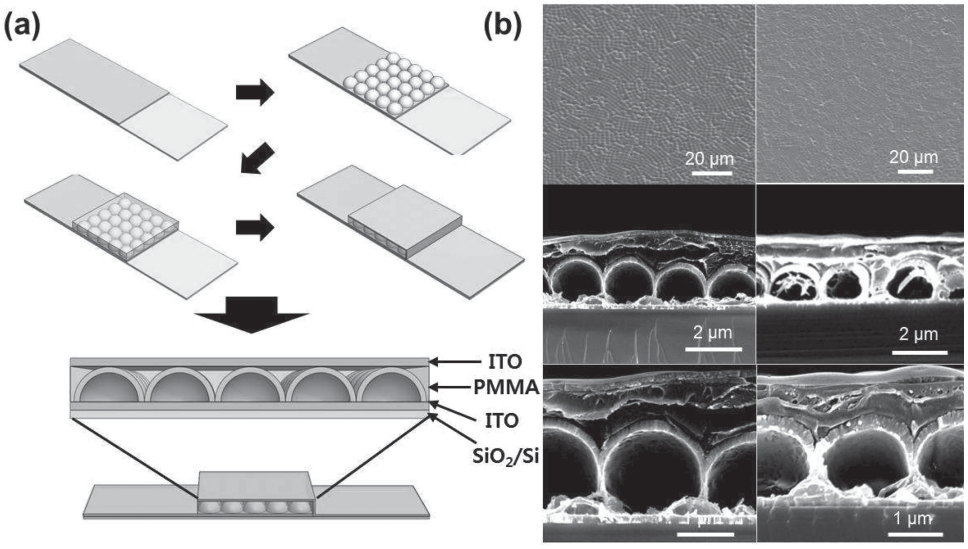

Figure 6. a) The schematic diagrams of the nanogenerator fabrication process. b) Low and high magnification SEM images of the nanogenerator.

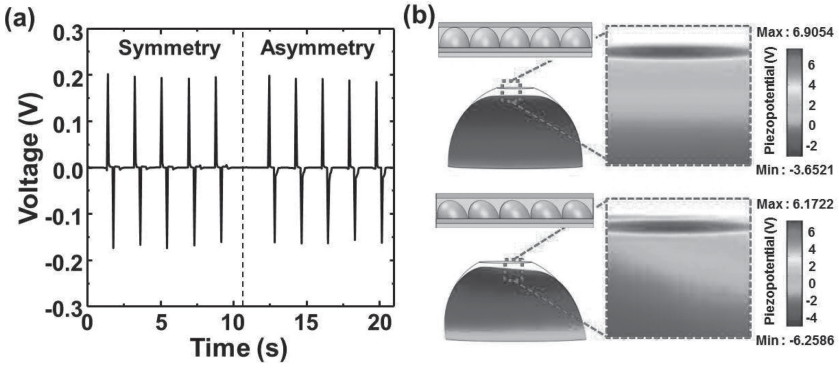

Figure 7. a) Open-circuit voltage and b) piezoelectric potential distributions of nanogenerators with symmetric (top) and asymmetric (bottom) hollow hemispheres.

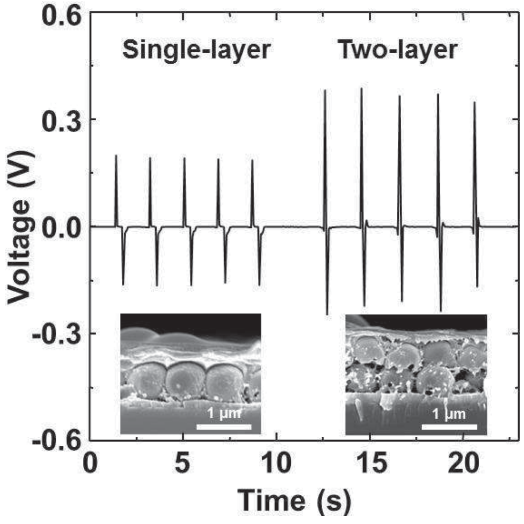

Figure 8. Open-circuit voltage of embossed thin film generator with single-layered and two-layered hollow hemispheres.

the change of current density of the sensor with the magnitude of applied force. It can be clearly seen that the change of the current density increased nearly linearly as the external force increased from 0.5 to 30 N for the ZnO embossed film.

On the contrary, it is seen that piezoelectric potential distributions are at the same level along the vertical direction, irrespective of the degree of symmetry. To verify it, we measured the output voltage of the embossed film-type nanogenerator, sandwiched between the top and bottom electrodes by pushing the film. As shown in **Figure 6**a, nanogenerator with this design has a four-layer structure. Figure 6b shows SEM images of the embossed ZnO thin film nanogenerator with symmetric and asymmetric hemispheres. The performance of the nanogenerator was then tested; the results are shown in **Figure 7**a. By pushing the nanogenerator, the embossed film with symmetric hemispheres repeatedly generates an open-circuit voltage of ≈0.2 V, which is the same voltage in embossed film with asymmetric hemispheres. The simulation results along the vertical direction are clearly seen in Figure 7b. A nanogenerator was also made by stacking two layers of such hemispheres layer-by-layer. It was done by spin-coating of the polystyrene on the hemispheres, followed by the deposition of ZnO film and post annealing. The layer-by-layer integrated nanogenerator shows the enhanced output voltage of ≈0.4 V as the sum of the output voltage of ≈0.2 V from the two individual hemispheres, as shown in **Figure 8**.

3. Conclusions

In summary, we reported ZnO embossed hollow hemispheres thin film for highly responsive pressure sensors and

piezoelectric nanogenerators. The asymmetric hemispheres, formed by an oblique angle deposition, caused an unsymmetrical piezoelectric field direction by external force, resulting in the control of the current direction and level at about 7 mA cm^{-2} at normal force of 30 N. The nanogenerators repeatedly generate the voltage output of ≈0.2 V, irrespective of the degree of symmetry. We also demonstrated that when one piece of hemisphere layer is stacked over another to form a layer-by-layer matched architecture, the output voltage in nanogenerators increases up to 2 times. This technique will make high-output nanogenerator possible.

4. Experimental Section

Production of ZnO Thin Films with Hollow Hemisphres: An aqueous suspension of 1-μm-diameter polystyrene beads (2.6 wt%, Polysciences, Warrington, USA) was used to prepare close-packed monolayer bead templates for the fabrication of embossed ZnO films, as described previously. Briefly, prior to spin-coating of the suspension on bare SiO_2/Si (for pressure sensors) and ITO-coated SiO_2/Si (for nanogenerators) substrates, the bare substrate was treated with UV/Ozone (AHTECH LTS, South Korea), making the surface of the substrate hydrophilic. A drop of polystyrene bead suspension was then pipette onto the SiO_2/Si substrate. Spin-coating of the polystyrene beads was done at 1300 rpm for 3 s, and then the sample was dried for 1 h in a dry box at room temperature. The spinning speed and slow drying were optimized because both were critical in obtaining monolayer bead templates without sphere-free regions or agglomeration. A 200-nm-thick ZnO film was deposited onto the substrates at room temperature by a RF sputtering, and it can be optimized further for a better device performance. The base pressure, working pressure, rf power, and gas flow rate were 1×10^{-6} Torr, 4 mTorr, 16/4 sccm (Ar/O_2), respectively. The hemispheres with asymmetric shapes were formed by OAD using a RF sputtering with a vapor flux angle of 85°. The samples were calcined in air at 300 °C for 60 min to burn out the polymer beads and simultaneously crystallize the ZnO film, resulting in an embossed ZnO film with hollow hemispheres on the substrate.

Fabrication of Pressure Sensors and Electrical Properties Measurement: For pressure sensors, laterally arranged Ti/Au (20/200 nm) electrodes were then deposited using electron beam evaporation at a base pressure of 3.0×10^{-6} Torr and bonded by Au wires (Figure 1a,b). The external force was applied by pushing the insulating Teflon block put on the embossed films. Exact values of applied force, by using a force testing system of Mecmesin Multitest i-1 (Slinfold, United Kingdom) were measured by using an electronic scale. *I–V* characteristics with the applied force were measured under air ambient using a Keithley 2636A source measurement unit.

Fabrication of Nanogenerator and the Measurement of Output Voltage: For nanogenerators, a layer of 2 μm thick poly(methyl methacrylate) (PMMA) was spin-coated on the embossed ZnO films. As a top electrode, ITO layer was then placed above the heads of the embossed ZnO films (Figure 6a,b). A nanogenerator was also made by stacking two pieces of the hemispheres. We measured the output voltages of the embossed thin film generators by applying a pushing force. To detect currents and voltages generated by Embossed thin film nanogenerator, a Keithley 6485 picoammeter and Keithley 2182A nanovoltmeter (R = 10 GΩ) were used.

Microstructural Analysis: The morphologies of the synthesized ZnO films were characterized by a Nano 230 field emission scanning electron microscope (FEI, USA). Transmission electron microscopy was performed using a transmission electron microscope (JEOL, Japan). A dual-beam focus ion beam (FEI, USA) was used to prepare the TEM samples. The crystalline properties of the films were characterized by a high resolution X-ray diffractometer (Bruker, Germany).

Acknowledgements

J.C. and K.Y.L. contributed equally to this work. This work was financially supported by the National Research Foundation of Korea (NRF) grant funded by the Ministry of Education, Science and Technology (MEST) (2012R1A2A1A01002787), the IT R&D program of MKE/KEIT [10035598, 180 lm/W High-efficiency nano-based LEDs], and by the Future Strategic Fund(1.130061.01) of UNIST(Ulsan National Institute of Science and Technology).

Received: August 24, 2013
Revised: October 3, 2013
Published online: November 19, 2013

[1] A. Hagfeldt, M. Gratzel, *Acc. Chem. Res.* **2000**, *33*, 269–277.
[2] M. K. Nazeeruddin, A. Kay, I. Rodicio, R. Humphrybaker, E. Muller, P. Liska, N. Vlachopoulos, M. Grätzel, *J. Am. Chem. Soc.* **1993**, *115*, 6382–6390.
[3] B. Oregan, M. Gratzel, *Nature* **1991**, *353*, 737–740.
[4] W. U. Huynh, J. J. Dittmer, A. P. Alivisatos, *Science* **2002**, *295*, 2425–2427.
[5] Q. B. Pei, G. Yu, C. Zhang, Y. Yang, A. J. Heeger, *Science* **1995**, *269*, 1086–1088.
[6] G. Yu, J. Gao, J. C. Hummelen, F. Wudl, A. J. Heeger, *Science* **1995**, *270*, 1789–1791.
[7] B. Z. Tian, X. L. Zheng, T. J. Kempa, Y. Fang, N. F. Yu, G. H. Yu, J. Huang, C. M. Lieber, *Nature* **2007**, *449*, 885–889.
[8] I. Gur, N. A. Fromer, M. L. Geier, A. P. Alivisatos, *Science* **2005**, *310*, 462–465.
[9] Y. Yang, W. Guo, K. C. Pradel, G. Zhu, Y. Zhou, Y. Zhang, Y. Hu, L. Lin, Z. L. Wang, *Nano Lett.* **2012**, *12*, 2833–2838.
[10] Z. L. Wang, J. H. Song, *Science* **2006**, *312*, 242–246.
[11] Z. L. Wang, *Sci. Am.* **2008**, *298*, 82–87.
[12] X. D. Wang, J. H. Song, J. Liu, Z. L. Wang, *Science* **2007**, *316*, 102–105.
[13] Y. Qin, X. D. Wang, Z. L. Wang, *Nature* **2008**, *451*, 809–813.
[14] R. S. Yang, Y. Qin, L. M. Dai, Z. L. Wang, *Nat. Nanotechnol.* **2009**, *4*, 34–39.
[15] S. Xu, Y. Qin, C. Xu, Y. Wei, R. Yang, Z. L. Wang, *Nat. Nanotechnol.* **2010**, *5*, 366–373.
[16] D. Choi, M.-Y. Choi, W. M. Choi, H.-J. Shin, H. K. Park, J. S. Seo, J. Park, S. M. Yoon, S. J. Chae, Y. H. Lee, S.-W. Kim, J.-Y. Choi, S. Y. Lee, J. M. Kim, *Adv. Mater.* **2010**, *22*, 2187–2192.
[17] K. Y. Lee, B. Kumar, J.-S. Seo, K.-H. Kim, J. I. Sohn, S. N. Cha, D. Choi, Z. L. Wang, S.-W. Kim, *Nano Lett.* **2012**, *12*, 1959–1964.
[18] S. Lee, J.-I. Hong, C. Xu, M. Lee, D. Kim, L. Lin, W. Hwang, Z. L. Wang, *Adv. Mater.* **2012**, *24*, 4398–4402.
[19] C. E. Chang, V. H. Tran, J. B. Wang, Y. K. Fuh, L. W. Lin, *Nano Lett.* **2010**, *10*, 726–731.
[20] S. Xu, B. J. Hansen, Z. L. Wang, *Nat. Commun.* **2010**,*1*.
[21] G. Zhu, A. C. Wang, Y. Liu, Y. Zhou, Z. L. Wang, *Nano Lett.* **2012**, *12*, 3086–3090.
[22] S. Lee, S.-H. Bae, L. Lin, Y. Yang, C. Park, S.-W. Kim, S. N. Cha, H. Kim, Y. J. Park, Z. L. Wang, *Adv. Funct. Mater.* **2012**, *23*, 2445–2449.
[23] L. Lin, Y. Hu, C. Xu, Y. Zhang, R. Zhang, X. Wen, Z. L. Wang, *Nano Energy* **2013**, *2*, 75–81.
[24] S. Lee, J.-I. Hong, C. Xu, M. Lee, D. Kim, L. Lin, W. Hwang, Z. L. Wang, *Adv. Mater.* **2012**, *24*, 4398–4402.
[25] Z.-H. Lin, Y. Yang, J. M. Wu, Y. Liu, F. Zhang, Z. L. Wang, *J. Phys. Chem. Lett.* **2012**, *3*, 3599–3604.
[26] S. Cha, S. M. Kim, H. Kim, J. Ku, J. I. Sohn, Y. J. Park, B. G. Song, M. H. Jung, E. K. Lee, B. L. Choi, J. J. Park, Z. L. Wang, J. M. Kim, K. Kim, *Nano Lett.* **2011**, *11*, 5142–5147.

[27] K. I. Park, S. Xu, Y. Liu, G.-T. Hwang, S.-J. L. Kang, Z. L. Wang, K. J. Lee, *Nano Lett.* **2010**, *10*, 4939–4943.
[28] J. M. Wu, C. Xu, Y. Zhang, Z. L. Wang, *ACS Nano* **2012**, *6*, 4335–4340.
[29] E. Strelcov, S. Dmitriev, B. Button, J. Cothren, V. Sysoev, A. Kolmakov, *Nanotechnology* **2008**, *19*, 355502.
[30] C.-H. Pan, H.-Y. Hsieh, K.-T. Tang, *Sensors* **2013**, *13*, 193–207.
[31] Y. Yang, L. Lin, Y. Zhang, Q. Jing, T.-C. Hou, Z. L. Wang, *ACS Nano* **2012**, *6*, 10378–10383.
[32] P.-H. Yeh, Z. Li, Z. L. Wang, *Adv. Mater.* **2009**, *21*, 4975–4978.
[33] Y. Yang, Y. Zhou, J. M. Wu, Z. L. Wang, *ACS Nano* **2012**, *6*, 8456–8461.
[34] W. Wu, X. Wen, Z. L. Wang, *Science* **2013**, *340*, 952–957.
[35] J.-T. Zhang, L. Wang, D. N. Lamont, S. S. Velankar, S. A. Asher, *Angew. Chem. Int. Ed.* **2012**, *51*, 6117–6120.